Supporting Materials: In Situ Studies on Phase Transitions of Tris(acetylacetonato)-Aluminum(Iii) Al(acac)$_3$

Nicole Pienack, Laura Ruiz Arana, Wolfgang Bensch and Huayna Terraschke *

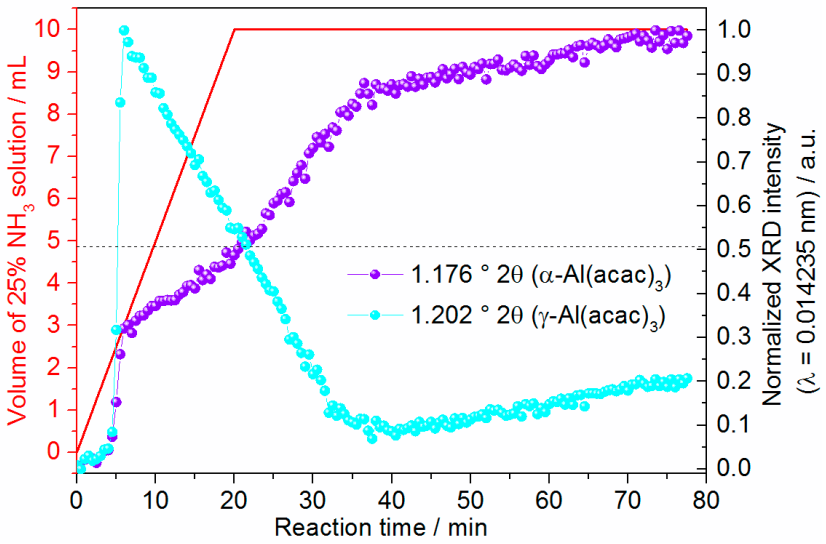

Figure S1. Dependence of the addition of 25% NH_3 solution as well as normalized intensity of the reflections (λ = 0.14235 Å) of α-Al(acac)$_3$ (1.176 ° 2θ) and γ-Al(acac)$_3$ (1.202 ° 2θ) on the reaction time, measured at the beamline P07B at DESY.

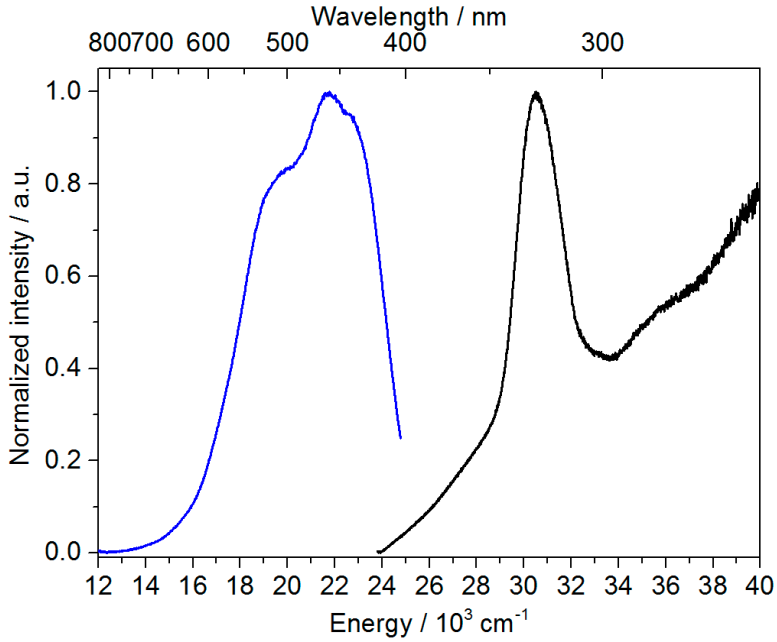

Figure S2. Emission (blue curve, λ_{ex} = 310 nm) and excitation (black curve, λ_{em} = 450 nm) spectra of Al(acac)$_3$, crystallized by the addition of 25% NH_3 solution.

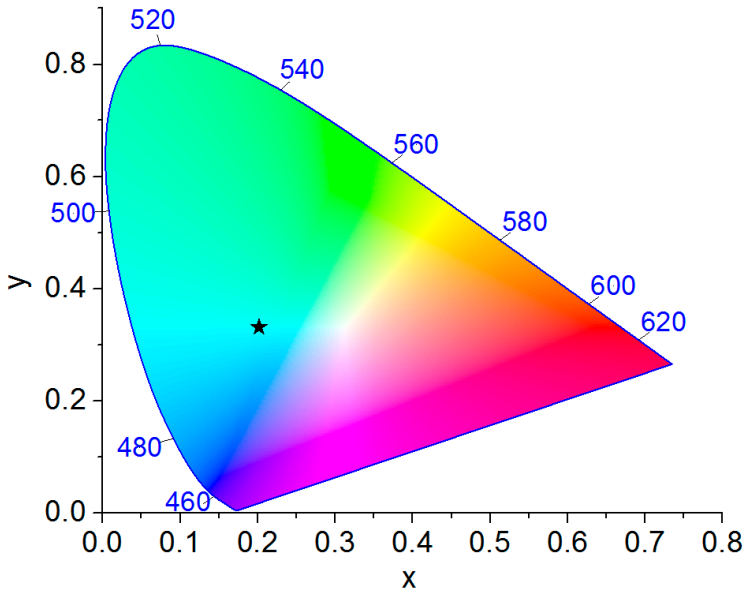

Figure S3. CIE (Commission Internationale de L'Éclairage) 1931 chromaticity diagram, displaying the color coordinated of $Al(acac)_3$ (x = 0.2017, y = 0.3313), calculated from the emission spectrum of Figure S2, applying the Spectra Lux Software v.2.0 [1].

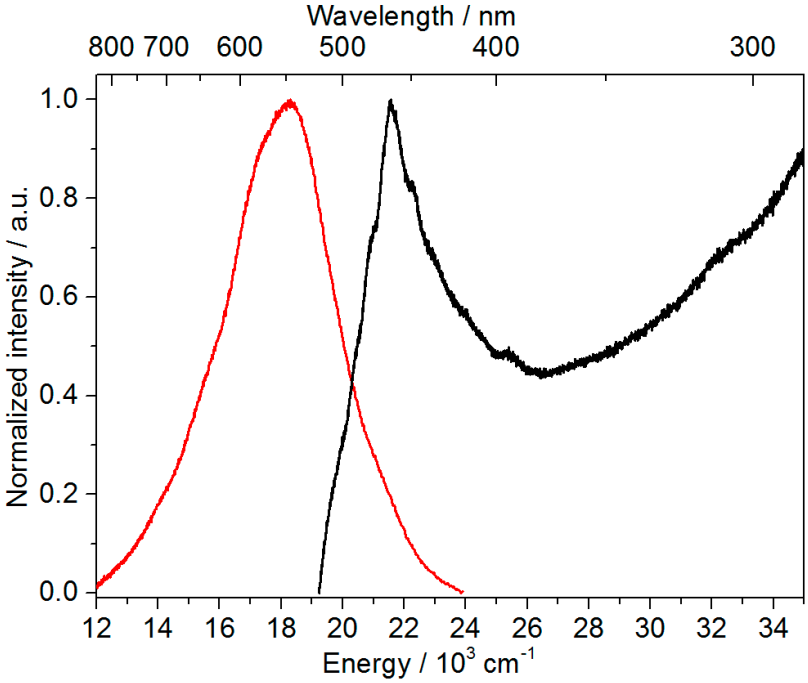

Figure S4. Emission (red curve, λ_{ex} = 380 nm) and excitation (black curve, λ_{ex} = 550 nm) spectra of pure acetylacetone.

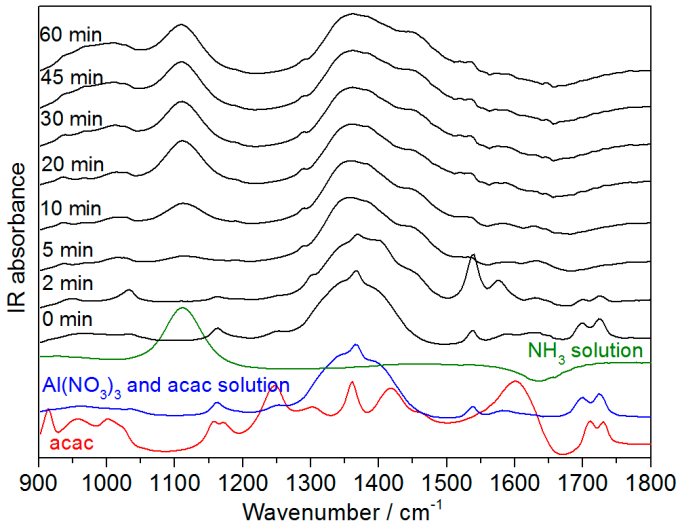

Figure S5. In situ IR spectra measured during crystallization with 25% NH_3 for reaction time t = 5–60 min, in comparison to starting solutions of NH_3 and aluminum nitrate with acetylacetone as well as pure acetylacetone.

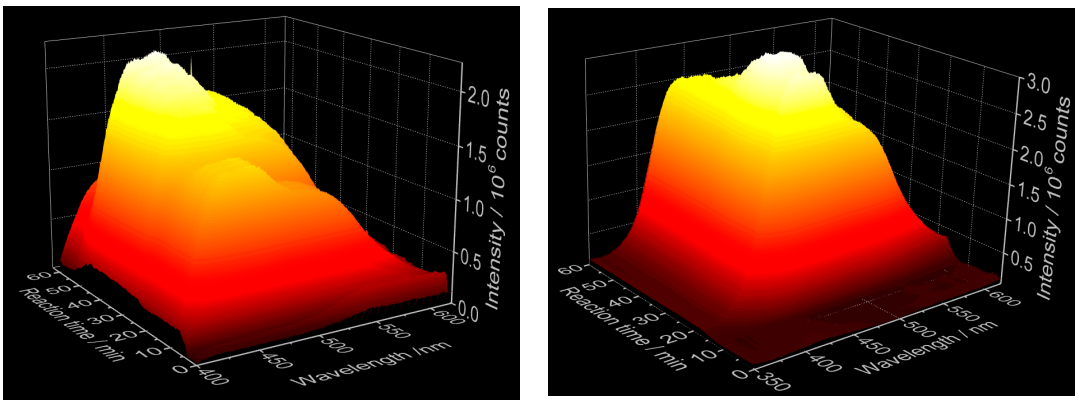

Figure S6. In situ luminescence spectra recorded during crystallization of $Al(acac)_3$ with (**a**) 12.5% and (**b**) 3.5% NH_3 solution (λ_{ex} = 320 nm).

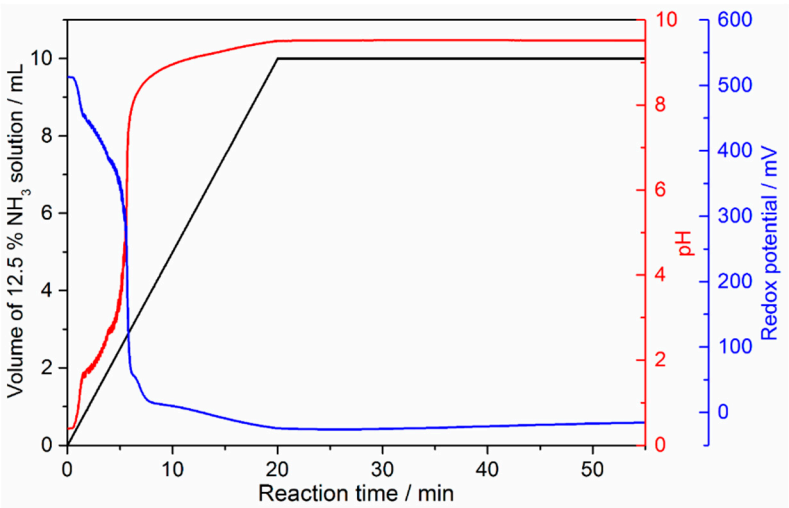

Figure S7. Dependence of the volume of 12.5% NH_3 solution (black curve), pH (red curve), and redox potential (blue curve) on the reaction time.

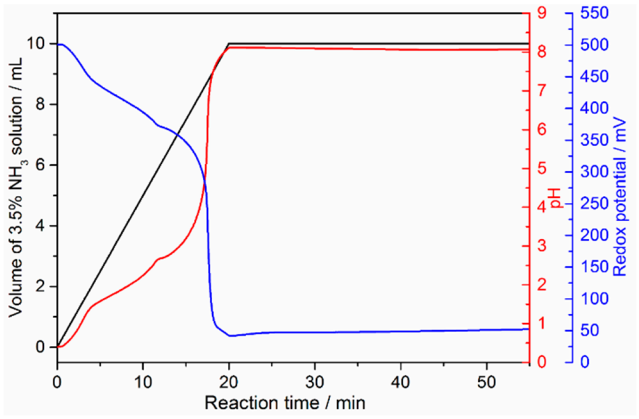

Figure S8. Dependence of the volume of 3.5% NH_3 solution (black curve), pH (red curve), and redox potential (blue curve) on the reaction time.

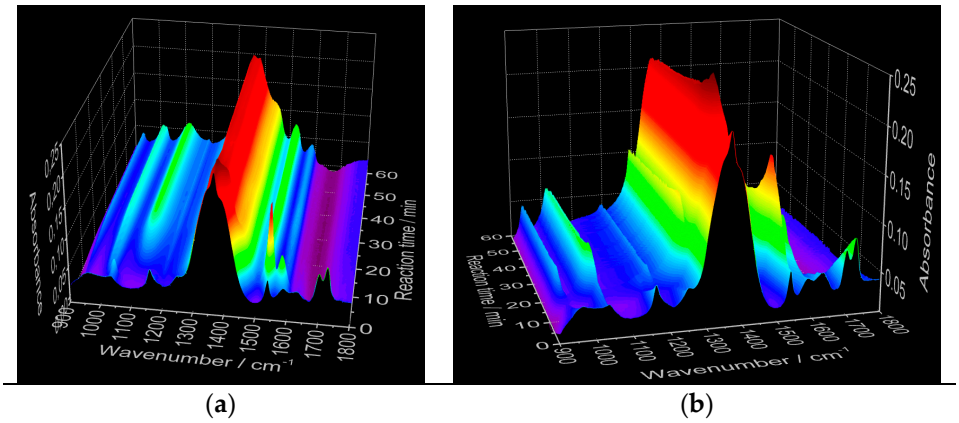

Figure S9. In situ IR spectra recorded during crystallization of Al(acac)3 with (**a**) 12.5% and (**b**) 3.5% NH_3 solution.

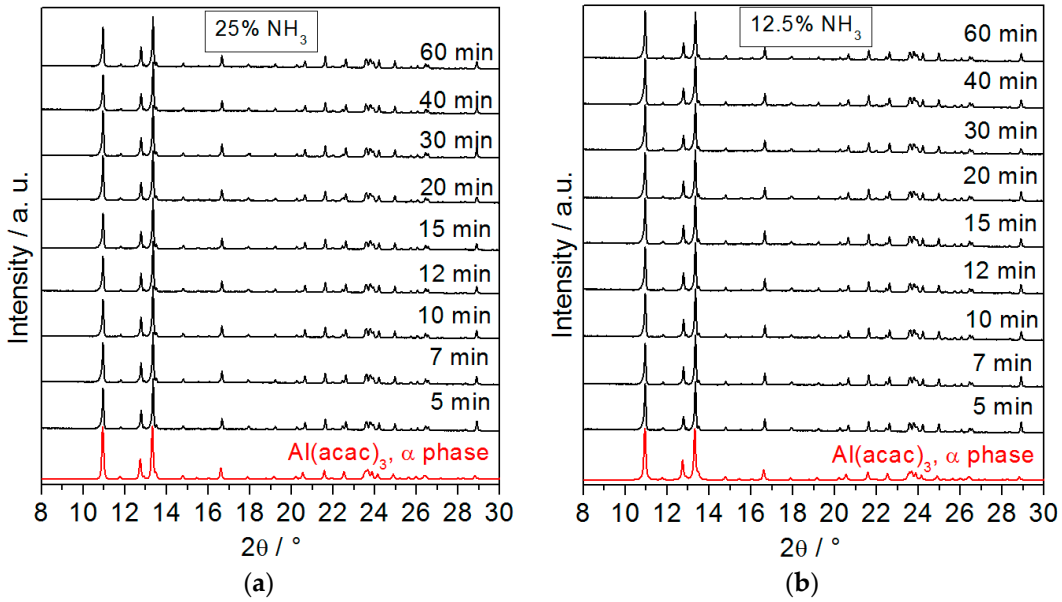

Figure S10. Ex situ XRD patterns of Al(acac)3 measured after the removal of the sample by reaction time t = 5–60 min, centrifuging and drying for reactions with (**a**) 25% NH3 and (**b**) 12.5% NH_3. Ex situ treatment causes complete conversion of the product to most stable α phases, showing the importance of in situ XRD measured with synchrotron radiation.

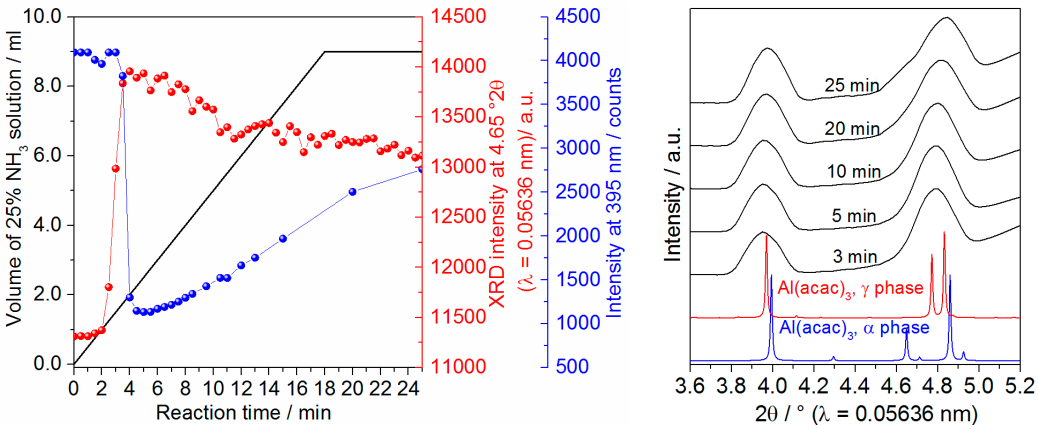

(**a**) (**b**)

Figure S11. Comparison of (**a**) light (blue curve) and XRD (red curve) intensity in dependence of the addition of NH_3 during crystallization of $Al(acac)_3$ and (**b**) comparison of measured in situ XRD patterns with calculated patterns for the respective α- and γ-phases.

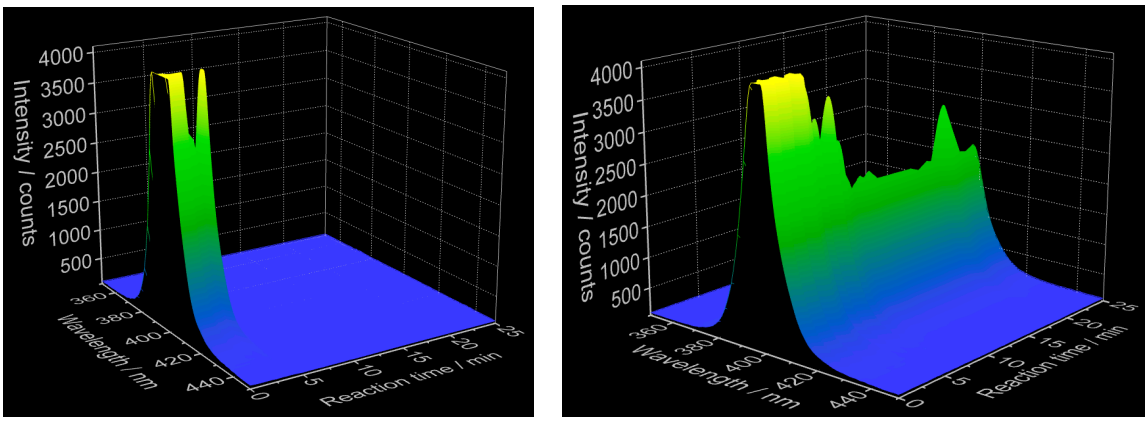

(**a**) (**b**)

Figure S12. (**a**) Light intensity of 395 nm LED transmitted through the reaction medium for the addition of (**a**) 12.5% NH_3 and (**b**) 2.5% NH_3 measured simultaneously to in situ XRD at the Beamline P09 at DESY. Oscillation of the light intensity is probably caused by mixing problems.

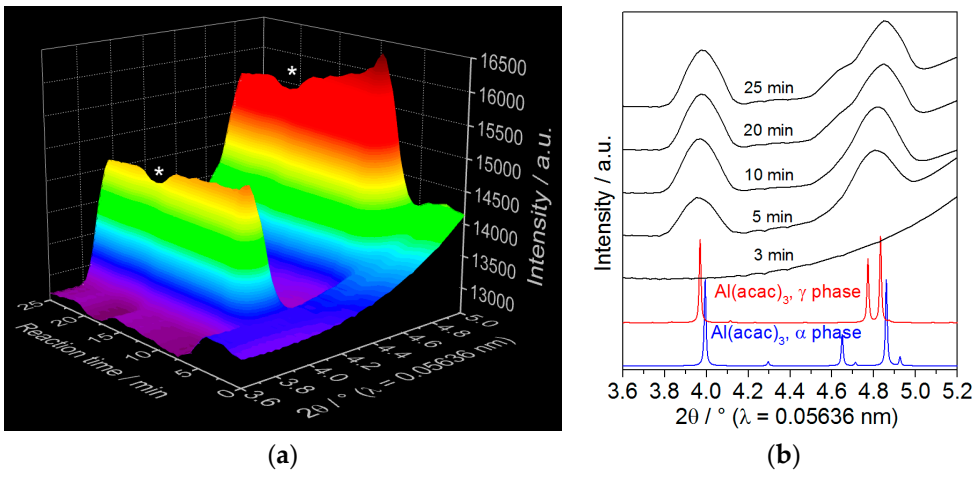

(**a**) (**b**)

Figure S13. (**a**) In situ XRD of $Al(acac)_3$ crystallized with a 12.5% NH_3 solution, measured at the Beamline P09 at DESY, and (**b**) comparison of measured in situ XRD patterns with calculated patterns for the respective α- and γ-phases. The asterisk (*) sign shows an artefact caused by the oscillation at the beam intensity.

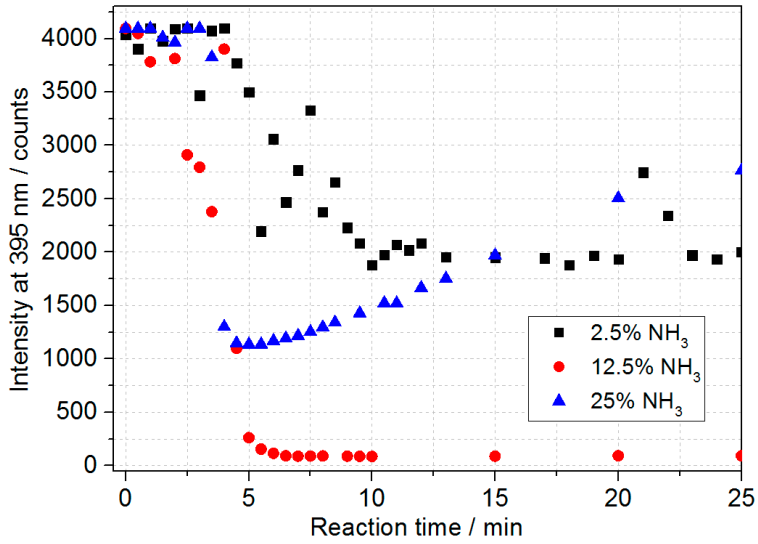

Figure S14. Comparison of light transmission intensity through the reaction solution for the crystallization of Al(acac)3 by the addition of 2.5%, 12.5%, and 25% NH3 solution.

The In Situ Crystallization Cell

The following figures should give an impression about the setup of the crystallization cell in our lab in Kiel (Figures S15 and S16), at the PETRA III beamline P07 (Figure S18) and the DORIS beamline F3 (Figure S19). The modified reaction vessel and the special sample holder are shown as well (Figure S17).

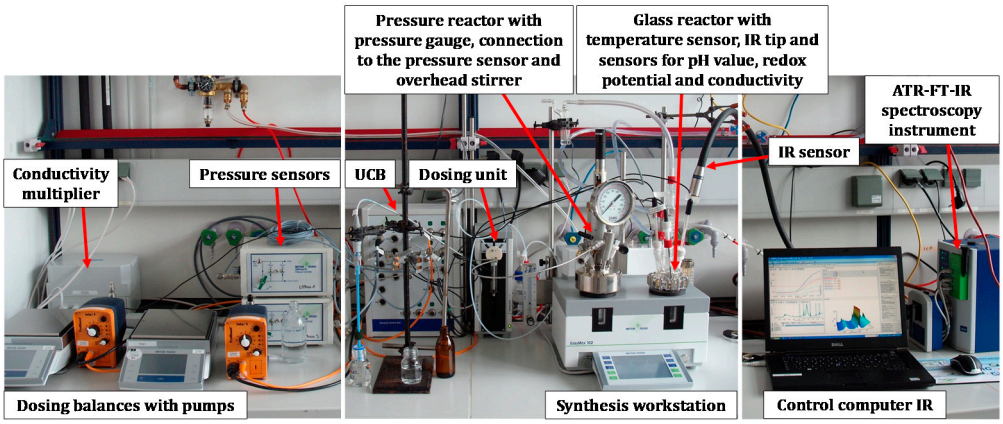

Figure S15. Setup of the crystallization cell in Kiel. The main parts of the equipment are marked.

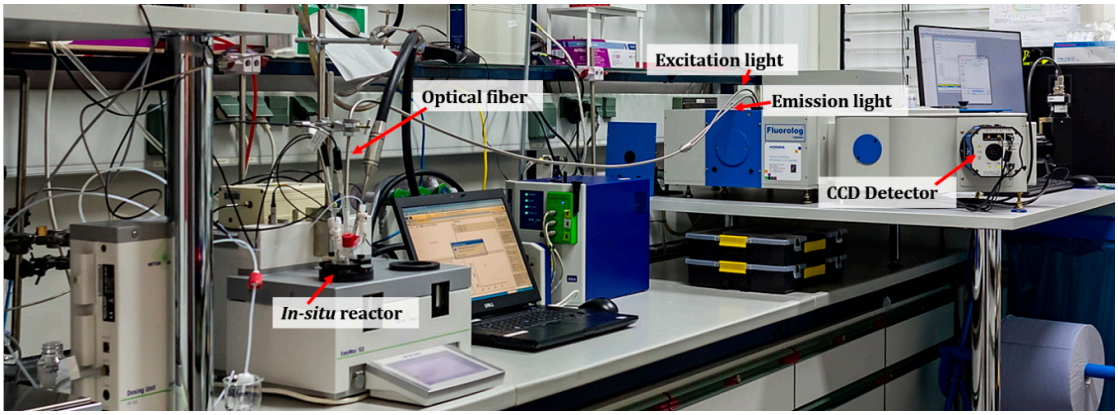

Figure S16. Adaptation of the crystallization cell in Kiel for in situ luminescence measurements.

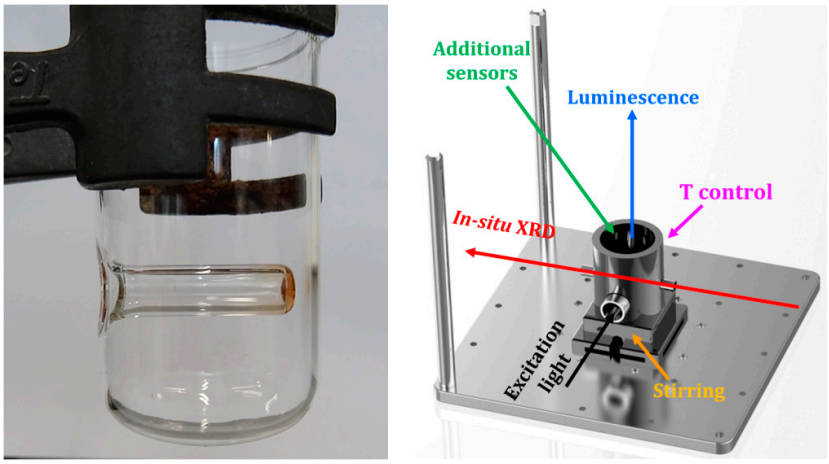

(**a**) (**b**)

Figure S17. (**a**) Modified reaction vessel with a glass tube fixed inside; (**b**) Scheme of the special constructed sample holder (for the glass vessel (**a**)) for temperature control, stirring, additional sensors, XRD, and luminescence measurements [2].

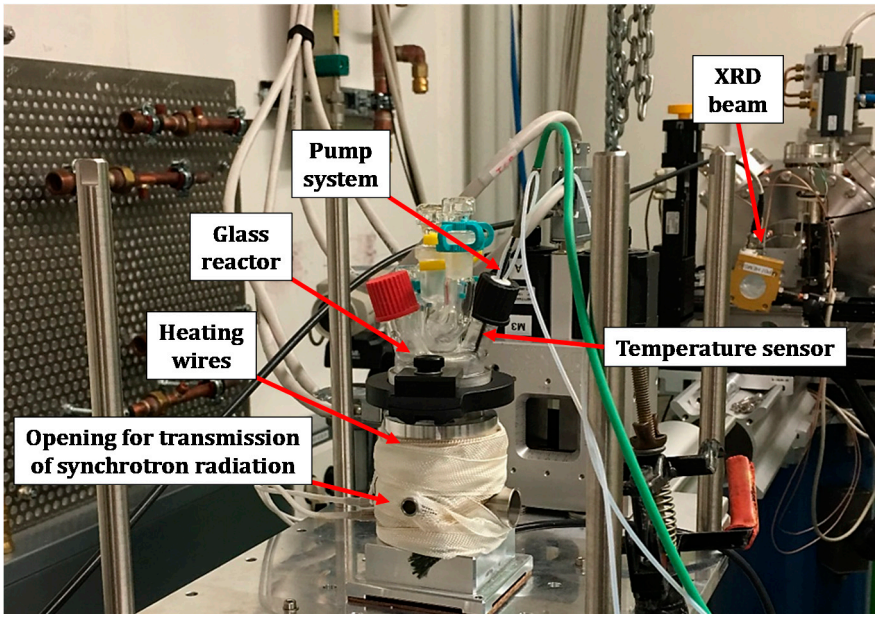

Figure S18. Experimental setup of the crystallization cell at the PETRA III beamline P07B, DESY, Germany. Here, the system is equipped with modified glass vessel for the scattering experiments (see figures below).

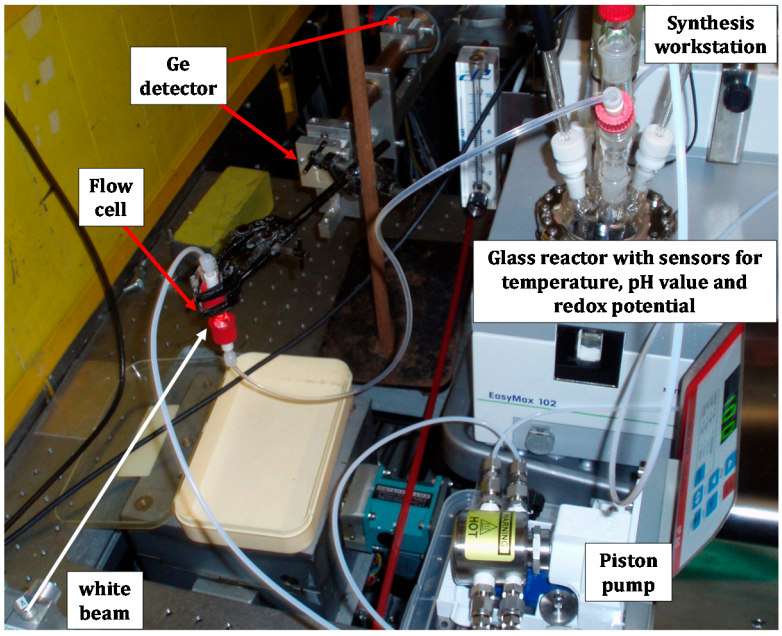

Figure S19. Experimental setup of the crystallization cell at the DORIS beamline F3, HASYLAB, DESY, Germany. Here, the system is equipped with an external flow cell for the scattering experiments and a piston pump allowing the circulation of the reaction mixtures.

References and Notes

1. Santa-Cruz, P.A.; Teles, F.S. *SpectraLux Software v. 2.0: Ponto Quântico Nano-Dispositivos/RENAMI*, Recife, Brazil, 2003.
2. Heidenreich, N. Unpublished Results. 2016.